Korean J. Chem. Eng., 35(11), 2157-2163 (2018)
DOI: 10.1007/s11814-018-0143-4

pISSN: 0256-1115
eISSN: 1975-7220

Tubular reactor design for the oxidative dehydrogenation of butene using computational fluid dynamics (CFD) modeling

Joseph Albert Mendoza and Sungwon Hwang†

Graduate School of Chemistry and Chemical Engineering, Inha University, 100 Inha-ro, Michuhol-gu, Incheon 22212, Korea
(*Received 29 May 2018 • accepted 23 August 2018*)

Abstract−Catalytic reactors have been essential for chemical engineering process, and different designs of reactors in multi-scales have been previously studied. Computational fluid dynamics (CFD) utilized in reactor designs have been gaining interest due to its cost-effective advantage in designing the actual reactors before its construction. In this work, butadiene synthesis via oxidative dehydrogenation (ODH) of *n*-butene using tubular reactor was used as a case study in the CFD model. The effects of coolant and reactor diameter were investigated in assessing the reactor performance. Based on the results of the CFD model, the conversion and selectivity were 86.5% and 59.5% respectively in a fixed bed reactor under adiabatic condition. When coolants were used in a tubular reactor, reactor temperature profiles showed that solar salt had lower temperature gradients inside the reactor than the cooling water. Furthermore, higher conversion (90.9%) and selectivity (90.5%) were observed for solar salt as compared to the cooling water (88.4% for conversion and 86.3% for selectivity). Meanwhile, reducing the reactor diameter resulted in smaller temperature gradients with higher conversion and selectivity.

Keywords: Catalysis, Computer Modelling, Heat Transfer, Kinetics, Reactor Design

INTRODUCTION

Hydrocarbons such as butene and butadiene have been known as essential raw materials in producing important industrial chemicals such as synthetic rubbers and plastics [1,2]. The global demand for these two chemicals increased consistently over the past decades [3,4]. Butadiene has been produced via three major synthesis routes: (a) steam cracking of hydrocarbons such as naphtha, (b) catalytic dehydrogenation of *n*-butane, and (c) oxidative dehydrogenation of *n*-butene [5]. Most of the total butadiene produced globally came from the naphtha catalytic cracking (NCC) process [6-8]. To date, cracking is the most popular method used to produce light olefins such as ethylene, propylene, and butene. NCC involves the breakdown of heavier hydrocarbons (C5-C12) into lighter hydrocarbons (C2-C4). It has been an energy-consuming process because of the highly endothermic reaction involved and the additional energy required to activate the reactants [9,10]. Ren et al. [11] reported high CO_2 emissions and coke depositions formed from the hydrocarbon pyrolysis as major environmental concerns for the cracking process. For this reason, researchers globally have called for a more efficient butadiene production that aimed to reduce overall CO_2 emissions and energy consumption. Meanwhile, catalytic dehydrogenation has a lower production cost and it is more environment-friendly than cracking [5,9]. Catalytic or direct dehydrogenation has been an alternative route for producing butadiene. This process has an unselective reaction and decomposes alkenes (or alkanes) into butadiene and hydrogen. However, this process was found to have obvious limitations: conversion and selectivity constraints due to its high endothermicity, multiple side reactions, rapid coke formation, and rapid catalyst deactivation [5]. To solve these limitations, oxidative dehydrogenation (ODH) process has been developed [12]. During the recent decades, ODH have been studied because it was found to efficiently produce butadiene with high selectivity and yield; and it does not suffer the same problems identified above affecting NCC and direct dehydrogenation [5]. ODH is an exothermic reaction and can be carried out at lower temperatures (*i.e.* 300-400 °C) than direct hydrogenation (*i.e.* 500-650 °C). The low reaction temperatures utilized for the ODH process can lead to substantial energy savings. Additionally, the presence of O_2 in the ODH process promotes coke combustion on the catalyst surface preventing catalyst deactivation [10]. However, ODH reaction has its limitation: the selectivity is hardly controllable and is strongly influenced by the reaction conditions used. Similar with naphtha cracking, ODH also produces many byproducts, which require additional separation unit processes. However, previous studies have been conducted to improve the selectivity and yield of butadiene at mild reaction conditions allowing for ODH process to compete with the existing NCC technology [13]. Developing novel and efficient catalysts were among the focus of previous researches in ODH [13,14]. Bismuth molybdates (Mo-Bi), ferrites, iron oxides, Cr_2O_3/Al_2O_3, vanadium-MgO composites, tin and antimony oxides, and carbon-based materials were studied previously as potential catalysts for the ODH process [3-5,8,14-16]. Ferrites and Mo-Bi have been the most widely used catalyst in the ODH process because it exhibited high catalytic activity and fewer byproducts [5, 14,17].

Optimal design of catalytic reactors has been another key research focus [18]. Designing reactors have been essential for chemi-

†To whom correspondence should be addressed.
E-mail: sungwon.hwang@inha.ac.kr

cal engineering processes including ODH. Various designs of catalytic reactors in multi-scales have been previously studied [19,20]. Three reactor types have been popular with the ODH reactions: adiabatic fixed-bed, fluidized bed, and isothermal multi-tubular reactor. Adiabatic fixed-bed reactor has the simplest design among reactor types and has good product yield and selectivity. However, adiabatic fixed-bed reactor does not have the ability to control temperature inside a reactor, resulting in more side products that require further separation processes. Meanwhile, fluidized bed reactor can have more uniform temperature distribution across a reactor due to good mixing, and it increases product yield and selectivity compared to the adiabatic fixed-bed reactor. However, complexity is much higher compared to other types of reactors in terms of design and operation. Also, performance of a reactor is heavily dependent on the size distribution of catalysts inside a reactor. Lastly, isothermal multi-tubular reactor, having a shell and tube configuration, has good control over the temperature across the reactor. Therefore, this type of reactor is well adopted for strong exothermic reactions such as ODH. In this reactor, coolants that flows co-currently or counter-currently are utilized to achieve isothermal conditions inside a reactor even though the regeneration or replacement of deactivated catalyst for this reactor can be rather challenging [14]. It was found that most ODH reactions occur at the inlet of the reactor resulting in rapid temperature increase. Meanwhile, the temperature inside a reactor needs to be maintained at the optimum level to maximize yield of main products avoiding also thermal runaway behavior. For this reason, it was found that tubular reactor with cooling medium is most appropriate for ODH reaction.

With the dawn of technology, computer-aided reactor modelling has gained worldwide attention mainly because of its cost-effective advantage in designing the actual reactors before its actual fabrication. Optimization of various design and operating parameters such as reactor length, gas flow rate, inlet temperature, *etc.* are essential to maximize reactor performance and efficiency. Computational fluid dynamics (CFD) were used to investigate the flow patterns within the reactor to understand heat and mass transfer, and its influence on chemical reaction kinetics. Various CFD models were developed depending on reactor types and configurations [21,22]. Discrete element method (DEM) coupled with CFD was used for fluidized bed reactor for olefin synthesis [23,24]. Another model was the energy minimization multi-scale (EMMS) model, which was used to describe multi-scale phenomenon in a gas-solid multi-phase catalytic reactor [25,26]. MATLAB and its optimization toolbox have been used to develop models for monolithic and multi-channel reactors [6]. It was used to develop the kinetic and mechanistic study for ODH using carbon catalysts [10]. Tian et al. [22] studied the effect of diameter-to-length configuration of the reactor for acetylene hydrogenation using CFD. Meanwhile, CFD coupled with a process modeling software was also used to model the effect of coolant (*i.e.* solar salt) flow rate and baffle configuration on the overall reactor performance for *o*-xylene conversion [19].

However, no previous studies have presented a comparative analysis between water and solar salt as a coolant for tubular reactors

Table 1. Chemical equations and kinetic parameters used in the CFD model [28]

Reaction	Pre-exponential factor	Activation energy ($J \cdot kmol^{-1}$)
$C_4H_8+\frac{1}{2}O_2 \rightarrow C_4H_6+H_2O$	6×10^{12}	5.02×10^{8}
$C_4H_8+6O_2 \rightarrow 4CO_2+4H_2O$	3×10^{7}	1.04×10^{7}
$C_4H_6+\frac{11}{2}O_2 \rightarrow 4CO_2+3H_2O$	3×10^{7}	1.04×10^{7}

Table 2. Reaction parameters and physical property parameters of the CFD model [12,23]

Parameter	Value
Inlet mole fractions	
-C_4H_8	0.06
-O_2	0.05
-H_2O	0.89
Operating pressure (Pa)	101,325
Inlet temperature (K)	633
Gas velocity ($m \cdot s^{-1}$)	0.05
Catalyst porosity	0.35
Catalyst density ($kg \cdot m^{-3}$)	1,919
Gas mixture density	Incompressible ideal gas law
Thermal conductivity of the catalyst ($W \cdot m^{-1} \cdot K^{-1}$)	0.2514
Heat capacity of the catalyst ($J \cdot g^{-1} \cdot K^{-1}$)	1,580
Heat transfer coefficient, solar salt ($W \cdot m^{-2} \cdot K^{-1}$)	1,600
Heat transfer coefficient, cooling water ($W \cdot m^{-2} \cdot K^{-1}$)	500
Particle diameter (mm)	3.0
Reactor inside diameter (cm)	2.54
Wall thickness (cm)	0.21
Surface-to-volume ratio (m^{-1})	3,000

in the ODH reaction of butene. Furthermore, the effect of varying the reactor configuration (*i.e.* diameter of tube) and coolant on exothermic reactions such as ODH were not widely discussed. Also, reaction kinetic parameters were hardly calibrated in CFD models to increase its accuracy because of the occasionally complex kinetic equations involved. In this work, the reaction kinetics were calibrated, and CFD modeling was utilized to investigate the effects of varying diameter of the reactor tube and type of coolant on the conversion and yield of the ODH reaction of butene.

MODEL DEVELOPMENT

1. Reactor Size and Geometry Used for the CFD Model

An isothermal multi-tubular fixed-bed reactor was chosen for the CFD model because of the high product yield and conversion among the reactor types described in the previous section. However, it was reduced to a single tubular reactor for simplification purposes similar to the models previously developed [12]. The reactor has a length of 32 in (81.28 cm) and an inside diameter of 1 in (2.54 cm) filled with the solid catalyst particles. In the CFD model, the reactor was drawn as a half cylinder assuming symmetry along the longitudinal plane. ANSYS Design Modeler and Meshing was used in creating the model geometry and mesh grids, while ANSYS Fluent performed the numerical solutions. Fluent utilizes finite volume method in solving governing equations of heat and mass transfers. Therefore, the geometry was discretized into small grids or cells. While there is an interdependency in the number of cells with the accuracy and the computation speed [23], the mesh grid created for the model to contain at least 5,000 cells was adequately accurate. Computation speed is dependent with the available computer hardware resources (*i.e.* processor speed, number of processor cores, memory, disk space, *etc.*). The model ran on a computer with an Intel Xeon® processor (2.10 GHz, 16 cores) and 64 GB of RAM which was enough for this study.

2. Kinetic Model

Typical oxidative dehydrogenation of *n*-butene involves gas-solid reaction systems occurring at active sites within the catalyst particles. Sterrett and McIlvried [12], Wgialla et al. [27], and Xingan and Huiqin [14] developed a kinetic model for the ODH reaction of butene to butadiene with ferrite catalysts. However, recent papers by Huang et al. [6] and Park et al. [10] revealed that the mechanism involves mostly reactant adsorption on the solid catalyst in an oxidative dehydrogenation, which is governed primarily by Mars-van Krevelen (MVK) theory. Therefore, in this CFD model, the kinetic model derived from the MVK theory was used. The activation energies and pre-exponential factors were specified in the Fluent interface.

3. Model Parameters

The model parameters such as pressure, temperature, catalyst properties (*e.g.* density, thermal conductivity, tortuosity factor, porosity, heat capacity, *etc.*), inlet/outlet boundary conditions, and governing equations (Table 1-3) were derived from the previous studies to develop the CFD model. Readers are advised to check the literatures [6,23,27] for the details of governing equations. Literature values were used [12,23] to validate our CFD model since these models had been confirmed with experimental data.

Table 3. Governing equations for the CFD model [23]

Gas phase continuity equation:

$$\frac{\partial(\phi\rho_g)}{\partial t}+\nabla\cdot(\phi\rho_g\vec{v})=0$$

Gas phase momentum equation:

$$\frac{\partial(\phi\rho_g\vec{v})}{\partial t}+\nabla\cdot(\phi\rho_g\vec{v}\vec{v})=-\phi\nabla p+\nabla\cdot\phi\bar{\bar{\tau}}+\phi\rho_g\vec{g}=\vec{S}$$

$$\bar{\bar{\tau}}=\mu\left[(\nabla\vec{v}+\nabla\vec{v}^{T})-\frac{2}{3}\nabla\cdot\vec{v}\bar{\bar{I}}\right]$$

$$\vec{S}=150\frac{(1-\phi)^2\mu}{d_p^2\phi^2}+1.75\frac{\rho_g(1-\phi)|\vec{v}|}{d_p^2\phi}\vec{v}$$

Gas phase equation of state:

$$p=\frac{\rho_g RT}{M}$$

Species conservation equation:

$$\frac{\partial(\phi\rho_g Y_i)}{\partial t}+\nabla\cdot(\phi\rho_g\vec{v}Y_i)=-\phi\nabla\cdot\vec{J}_i+\phi r_i\ \{i\in(1,N_r)\}$$

$$\vec{J}_i=-\rho_g D_{i,eff}\cdot\nabla Y_i$$

$$D_{i,eff}=\frac{\varepsilon}{\tau}\frac{1}{\left(\frac{1}{D_{i,m}}+\frac{1}{D_{i,k}}\right)}$$

$$D_{i,k}=97\frac{d_0}{2}\sqrt{\frac{T}{M_i}}$$

$$D_{i,m}=\frac{1-Y_i}{M\Sigma_{\substack{j=1\\ j\neq i}}^{n}\left(\frac{Y_j}{M_j D_{ij}}\right)}$$

$$D_{ij}=\frac{1.43\times10^{-3}\cdot T^{1.75}}{PM_{ij}^2[(\Sigma_v)_i^{1/3}+(\Sigma_v)_j^{1/3}]^2}$$

Mass rate of reaction:

$$r_i=M_i\sum_{r=1}^{N_r}\left[(v''_{i,r}-v'_{i,r})\left(k_r\prod_{j=1}^{N_r}(C_{j,r})^{(\eta'_{j,r}+\eta''_{j,r})}\right)\right]$$

Energy equation:

$$\frac{\partial(\phi\rho_g E_g+(1-\phi)\rho_{cat}E_s)}{\partial t}+\nabla\cdot(\vec{v}\rho_g E_g+p)$$
$$=\nabla\left[k_{eff}\nabla T-\left(\sum_{i=1}^{N_r}h_i\vec{J}_i\right)+\bar{\bar{\tau}}\cdot\vec{v}\right]+S_f^h$$

$$k_{eff}=\phi k_g+(1-\phi)k_s$$

4. Modeling Method

The CFD model was developed using Fluent 19.1 (ANSYS Inc., USA) with the double precision mode activated. To setup the CFD model, the appropriate model parameters (for catalyst and coolant) were specified on the FLUENT interface. Then, the solution method was set similar to Huang et al. [23] to ensure accuracy and convergence.

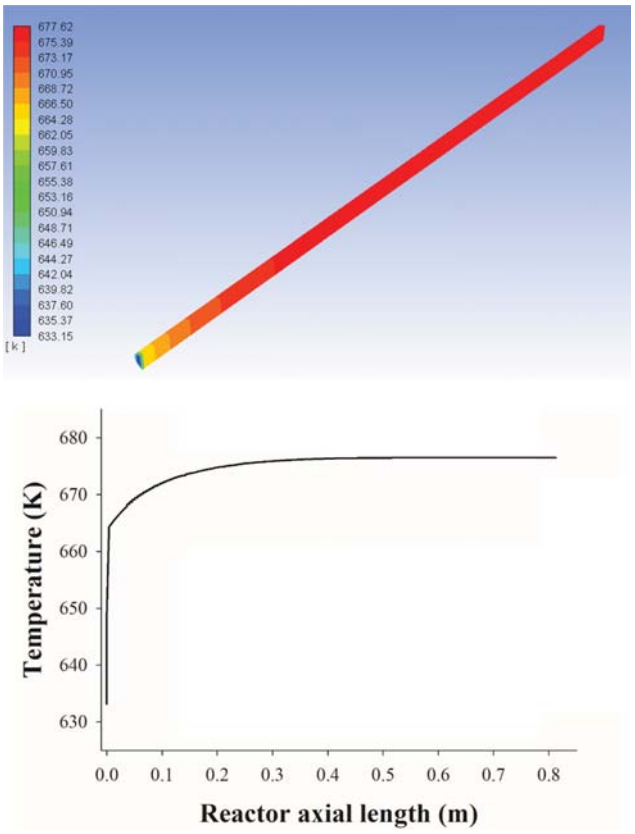

Fig. 1. Adiabatic temperature contour profile of the reactor along the reactor axial length.

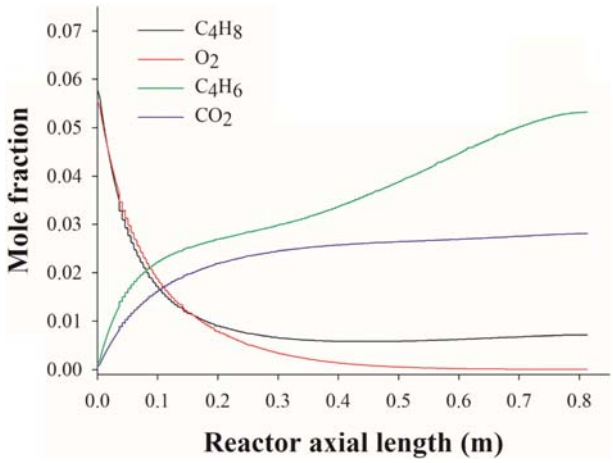

Fig. 2. Mole fraction concentration profile of butene, oxygen, butadiene, and CO_2 under adiabatic conditions.

RESULTS AND DISCUSSION

1. Operating the Reactor in Adiabatic Condition

ODH processes using fixed-bed reactors are usually operated adiabatically, and no coolant is utilized. First, adiabatic conditions were simulated in CFD to describe the temperature distribution in the reactor. The pressure drop in the reactor was negligible similar to previous literatures [23], and the process can be assumed isobaric. The velocity was maximum at the axial direction of the reactor, and it approaches zero at the radial direction because of the fixed wall boundary condition set for the CFD model. It is also assumed that there is no reaction at the reactor wall surface [29]. The temperature increased along the axial length of the reactor (Fig. 1). The temperature increased from 633 K to 665 K at the reactor inlet and gradually increased until it reached the maximum temperature (677 K). It was observed that the temperature is relatively constant at both radial and axial directions except at the reactor inlet as it was mentioned in previous literature [12]. The computational burden can be reduced if the accuracy of the model is rather relaxed at the rest of the reactor except at the inlet section. Furthermore, it is recommended that the length of the reactor should be decreased because the previous study presented very long reactor length for the reaction.

The concentration profile of the reactants and products is shown in Fig. 2. It is shown how C_4H_8 and O_2 are consumed (and conversely, C_4H_6 and CO_2 are formed) as the reaction proceeds along the reactor length, and the species concentrations had been uniformly distributed. This shows that the reaction is occurring on a laminar flow in the porous media and that turbulence can be neglected [6,23]. Under adiabatic conditions, the butene conversion and butadiene selectivity were 86.5% and 59.5%, respectively. Adiabatic condition favoured the CO_2 formation affecting overall yield of butadiene. However, the results obtained from this CFD model differed with the experimental results previously reported [12] under adiabatic conditions. This could be due to the reaction kinetics applied to the CFD model. The nonlinear reaction kinetics developed previously [12,14,27] produced diverging solutions when applied to the CFD model. However, a pseudo-first order reaction kinetics previously reported by Huang et al. [23] and Hong et al. [5] resulted in converging solutions. Therefore, a simplified reaction kinetics was enough to simulate the ODH reaction instead of the more complicated kinetics mentioned above. The oxidative dehydrogenation kinetics is dependent on the adsorption of the reacting species on the catalyst surface. However, the effect of adsorption was assumed to be negligible in the model for simplification purposes.

The kinetic model is crucial for the accuracy of the CFD model. To increase the accuracy of the CFD model, the reaction rate calculated from the previous model [23] was used as an initial parameter to calibrate the rate constants of the reactions. Then, the kinetic parameters were fitted for a good agreement between the simulated and experimental data. These values are shown in Table 4. This simplifies the reaction equation for the CFD model because the calibrated rate constant has incorporated the intraparticle diffusion and adsorption effects into one explicit parameter.

Table 4. Calibrated kinetic parameters used in the CFD model

Reaction	k_n, rate constant ($m^3 \cdot kmol^{-1} \cdot s^{-1}$)
(1) $C_4H_8+\frac{1}{2}O_2 \rightarrow C_4H_6+H_2O$	2.530×10^3
(2) $C_4H_8+6O_2 \rightarrow 4CO_2+4H_2O$	88.25
(3) $C_4H_6+\frac{11}{2}O_2 \rightarrow 4CO_2+3H_2O$	38.52

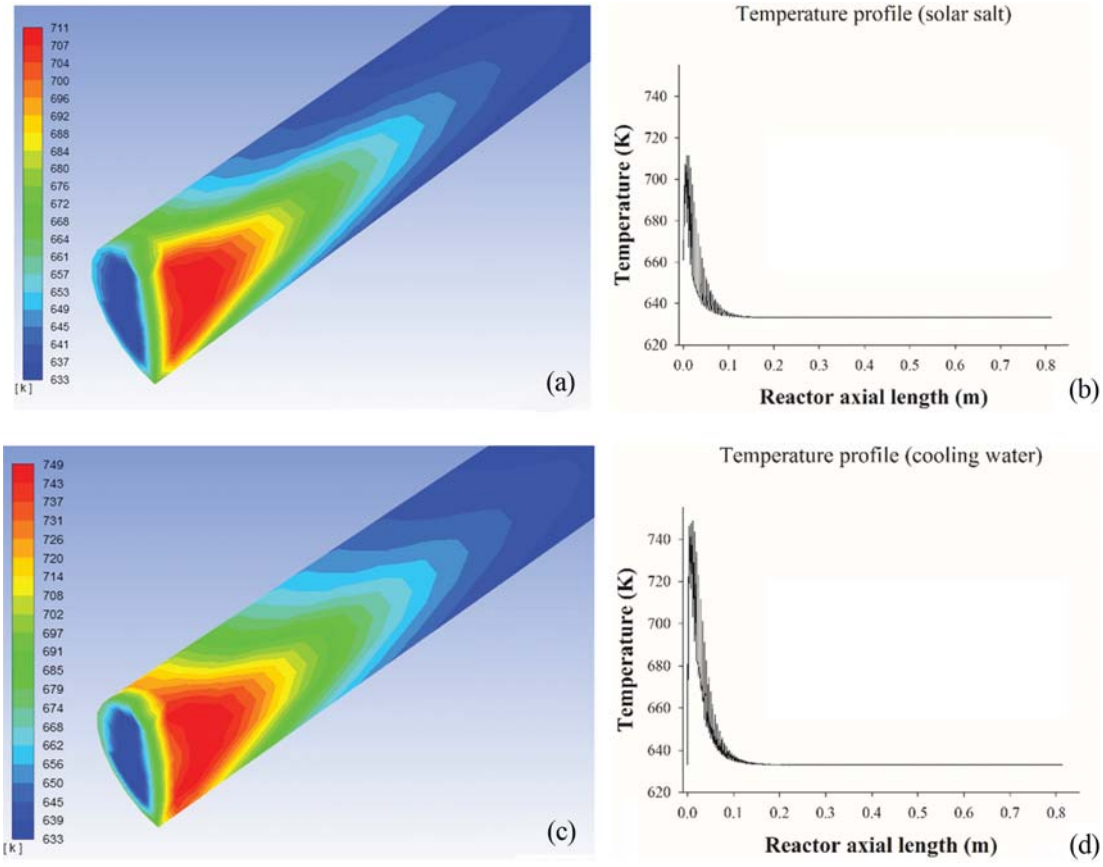

Fig. 3. Temperature contour profile of solar salt (a)-(b) and cooling water (c)-(d) along the reactor axial length.

2. Effect of Coolant: Comparing between Water and Solar Salt

Coolants are usually employed when multi-tubular packed bed reactors are utilized for the ODH process. Solar salts, which are a mixture of $NaNO_3$ and KNO_3 (60 : 40 w/w%), and water are usually employed as coolants in the ODH process. In this study, the effect and performance of these coolants were evaluated. The two coolants were compared and analyzed using the CFD model. Based on the results on Fig. 3, the solar salt provides better cooling capabilities than cooling water. Lower temperatures were observed on the reactor walls with solar salts than with the cooling water because of the higher heat transfer coefficient of solar salts compared to cooling water. High heat transfer coefficient is a characteristic of an efficient coolant [30]. Therefore, in the succeeding simulations, solar salts were used as the coolant in the CFD model. The coolant was assumed to be flowing co-currently with the reacting species for model simplification. However, the temperature increased above 700 K at the center of the reactor. The observed ΔT was greater than that obtained from the adiabatic condition, which can be due to the heat inhibition effect of the coolant. The reaction has mainly occurred at the reactor center, while the overall temperature in the reactor maintained at 633 K. The butene conversion and butadiene selectivity were 90.9% and 90.5%, respectively for solar salt. Meanwhile for cooling water, the conversion and selectivity were 88.4% and 86.3%, respectively. The conversion and selectivity improved when coolant was used compared to the adiabatic condition. Introducing coolant to the reactor minimized CO_2 formation and favored butadiene formation because of the decreased temperature gradient inside the reactor. Therefore, using coolants on tubular reactors was found to be advantageous in increasing conversion and selectivity of chemical processes [19]. From economic point of view, solar salts are relatively expensive compared with cooling water, which can add up to the operating costs for the reactor. Furthermore, it requires higher capital cost to install utility system for the supply of solar salt to the plant. On the other hand, the use of solar salts can increase performance of a reactor such as yield of main products. Therefore, these factors need to be considered before arriving at an optimized tradeoff between the two coolants. It should be also noted that the economic analysis can be performed once size of the plants, ratings of main equipment, required amounts of utilities are initially clarified, and the economic analysis should be performed repeatedly as the project progresses with updated data.

Another aspect to look upon to reduce cost would be optimizing the reactor size. For the ODH process, the reaction occurred mostly at the reactor inlet due to the location where the highest temperature difference was observed. After approximately 10 cm of the reactor length, the temperature started to equilibrate signifying that the reaction was approaching to its culmination. Therefore, the reactor length was decreased from 81.28 cm to 30 cm following the reactor model of Huang et al. [23]. After validating that the CFD model developed matched (Table 5), it has been utilized in the succeeding simulation analyzing the effect of varying

Table 5. Comparison of the CFD model in this study and the previous literature

	Conversion	Selectivity	Yield
Literature [23]	86.63%	0.74	63.85%
CFD model (this study)	86.80%	0.72	62.24%
% Error	0.20%	2.7%	2.5%

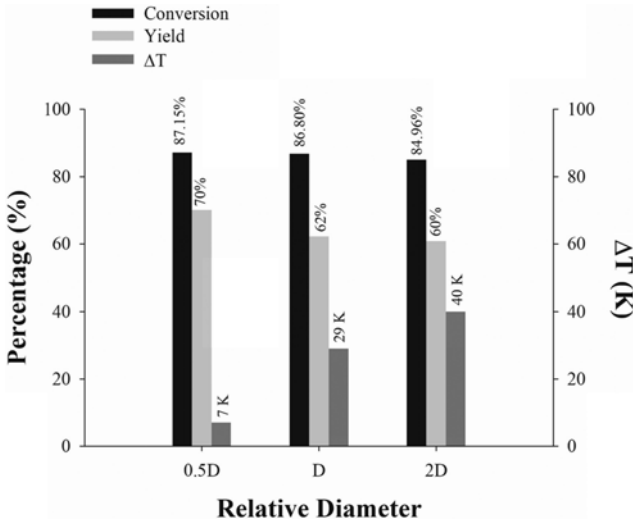

Fig. 4. Comparison of the conversion, yield, and ΔT with varying reactor diameters.

the reactor diameter.

3. Effect of Varying Reactor Diameter on Conversion and Temperature Profiles

The reactor diameter affects the conversion and temperature profiles based on the CFD results. Smaller diameter has higher conversion and yield than larger diameter (Fig. 4). It can be also noticed that the temperature difference (ΔT) was increasing as the reactor diameter is increased. Therefore, it can be concluded that the higher surface area-volume ratio provided more efficient heat transfer across the radial surface of the reactors for small reactor diameters. This resulted in lower ΔT on the reactor. Lower ΔT favored higher butadiene yield. Therefore, using smaller reactor diameter is more favorable to utilize than larger reactor diameter in terms of product yield. However, using smaller reactor diameter will result in increased number of equivalent reactor tubes, while maintaining the total reactor volume as compared to larger reactor diameter that could affect the overall capital cost of multitubular reactors. It can be presumed that the small reactor diameter can be suitable for oxidation reactions (*i.e.* ODH of butene) because of the low ΔT inside the reactor, which minimizes the undesired product formation. The lower temperature gradient inside the reactor could potentially reduce the coolant mass required to cool the reactor. Minimizing the reactor diameter can be more beneficial than increasing it. However, as previously mentioned, one must come up with an optimized tradeoff accounting for all possible scenarios including the reaction mechanism and kinetics involved before deciding on the proper reactor configuration.

CONCLUSIONS

This study presents a CFD model for the reactor design of ODH process of *n*-butene to 1,3-butadiene under both adiabatic conditions and operations with a flowing coolant. Concentrations of the reactant and product species, temperature, velocity, and pressure profiles in the reactor can be visualized using the CFD model. The corresponding CFD model was validated and compared with previous literatures. Based on the results, the butene conversion and butadiene selectivity were 86.5% and 59.5%, respectively, under adiabatic conditions. The reaction kinetics for ODH followed a simple pseudo-first order reaction. Therefore, the reaction of butene with the catalyst depends on the adsorption of butene on the catalyst surface. Then, the model was used to analyse the effect of coolant types on the overall reactor performance such as investigating the temperature profiles inside the reactor, butene conversion, and butadiene selectivity. Solar salts performed more efficiently than cooling water in decreasing the overall temperature gradient and improving the butadiene yield. This could be due to the higher heat transfer coefficient of solar salt than that of cooling water. In addition, the effect of reactor diameter was investigated. Increasing the reactor diameter, increases the temperature gradient, but decreasing the conversion and yield. However, using smaller reactor tube diameter would result in greater number of equivalent reactor tubes to maintain the total reactor volume. A reactor is considered as the core in terms of the process design, and how the reactor is designed can decide the rest of process designs such as separation and treatment systems. As described in this work, the use of smaller diameter and solar salt as coolant can increase performance of the reactor and reduce the overall costs for separation and treatment systems, while it requires higher capital cost for the reactor itself. Furthermore, it might require higher capital cost to install utility system for the supply of solar salt to the plant compared with cooling water system. Therefore, these factors need to be considered before arriving at an optimized tradeoff between the two coolants and size of the tubes inside the reactor. It should be also noted that the economic analysis can be performed once size of the plants, ratings of main equipment, and required amounts of utilities are initially clarified, and the economic analysis should be performed repeatedly as the project progresses with updated data.

ACKNOWLEDGEMENTS

This work was supported by INHA UNIVERSITY Research Grant.

NOMENCLATURE

$C_{j,r}$: concentration of the species [kmol/m^3]
$D_{i,eff}$: effective diffusion coefficient [m^2/s]
$D_{i,k}$: Knudsen diffusion coefficient [m^2/s]
$D_{i,m}$: Fickian diffusion coefficient [m^2/s]
d_0 : catalyst average diameter [m]
E_g : total fluid energy [kg/m^2/s^2]
E_s : total solid medium energy [kg/m^2/s^2]
$\vec{g}$: gravitational accelaration vector [m^2/s]

h_i : heat transfer coefficient [W/m^2/K]
$\vec{J}_i$: species diffusion flux i [kg/m^2/s^2]
k_g : gas phase thermal conductivity [W/K/s]
k_s : solid medium thermal conductivity [W/K/s]
k_{eff} : effective thermal conductivity of the medium [W/K/s]
k_r : rate constant
M_i : molar mass of *i*th component [kg/kmol]
N_r : number of chemical species
p : pressure [Pa]
r_i : reaction rate [kmol/m^3/s]
R : ideal gas constant [J/kmol/K]
$\vec{S}$: source term for the momentum equation [kg/m^3/s]
S_f^h : fluid enthalpy source term [J/m^3/s]
T : temperature [K]
$\vec{v}$: gas velocity vector [m/s]
Y_i : mass fraction of the *i*th component
ε : catalyst porosity
τ : Tuortosity
$v'_{i,r}$: stoichiometric coefficient for reactant
$v''_{i,r}$: stoichiometric coefficient for product
$\eta'_{j,r}$: rate exponent of the reactant species
$\eta''_{j,r}$: rate exponent of the product species
ρ_{cat} : catalyst density [kg/m^3]
ρ_g : mixture gas density [kg/m^3]
$\bar{\bar{\tau}}$: gas phase shear stress [Pa]
ϕ : bed porosity

REFERENCES

1. J.-H. Park and C.-H. Shin, *J. Ind. Eng. Chem.*, **21**, 683 (2015).
2. J.-H. Park, H. Noh, J. W. Park, K. H. Row, K. D. Jung and C.-H. Shin, *Res. Chem. Intermed.*, **37**, 1125 (2011).
3. J. Rischard, R. Franz, C. Antinori and O. Deutschmann, *AIChE J.*, **63**, 43 (2017).
4. H. Lee, J. C. Jung, H. Kim, Y.-M. Chung, T. J. Kim, S. J. Lee, S.-H. Oh, Y. S. Kim and I. K. Song, *Catal. Commun.*, **9**, 1137 (2008).
5. E. Hong, J.-H. Park and C.-H. Shin, *Catal. Surv. Asia*, **20**, 23 (2016).
6. K. Huang, L. Wang, S. Lin, Y. Xu and D. Wu, *J. Taiwan Inst. Chem. Eng.*, **63**, 61 (2016).
7. J.-H. Park and C.-H. Shin, *Appl. Catal., A*, **495**, 1 (2015).
8. W. Yan, Q. Y. Kouk, J. Luo, Y. Liu and A. Borgna, *Catal. Commun.*, **46**, 208 (2014).
9. J. H. Zhang, Z. B. Wang, H. Zhao, Y. Y. Tian, H. H. Shan and C. H. Yang, *Appl. Petrochem. Res.*, **5**, 255 (2015).
10. S. Park, Y. Lee, G. Kim and S. Hwang, *Korean J. Chem. Eng.*, **33**, 3417 (2016).
11. T. Ren, M. K. Patel and K. Blok, *Energy*, **33**, 817 (2008).
12. J. S. Sterrett and H. G. McIlvried, *Ind. Eng. Chem. Process Des. Dev.*, **13**, 54 (1974).
13. E. V. Makshina, M. Dusselier, W. Janssens, J. Degreve, P. A. Jacobs and B. F. Sels, *Chem. Soc. Rev.*, **43**, 7917 (2014).
14. W. Xingan and L. Huiqin, *Ind. Eng. Chem. Res.*, **35**, 2570 (1996).
15. F. J. Dumez and G. F. Froment, *Ind. Eng. Chem. Process Des. Dev.*, **15**, 291 (1976).
16. D. L. Trimm and D. S. Gabbay, *Trans. Faraday Soc.*, **67**, 2782 (1971).
17. J.-H. Park and C.-H. Shin, *Korean J. Chem. Eng.*, **33**, 823 (2016).
18. A. Heidari and S. H. Hashemabadi, *J. Taiwan Inst. Chem. Eng.*, **45**, 1389 (2014).
19. E. J. Hukkanen, M. J. Rangitsch and P. M. Witt, *Ind. Eng. Chem. Res.*, **52**, 15437 (2013).
20. H. Asadi-Saghandi and J. Karimi-Sabet, *Korean J. Chem. Eng.*, **34**, 1905 (2017).
21. R. I. Singh, A. Brink and M. Hupa, *Appl. Therm. Eng.*, **52**, 585 (2013).
22. L. Tian, G. Hu, W. Du and F. Qian, *Can. J. Chem. Eng.*, **94**, 2427 (2016).
23. K. Huang, S. Lin, J. Wang and Z. Luo, *J. Ind. Eng. Chem.*, **29**, 172 (2015).
24. J. T. Cornelissen, F. Taghipour, R. Escudié, N. Ellis and J. R. Grace, *Chem. Eng. Sci.*, **62**, 6334 (2007).
25. X. Liu, S. Hu, Y. Jiang and J. Li, *Chem. Eng. J.*, **278**, 492 (2015).
26. A. Bakshi, C. Altantzis, L. R. Glicksman and A. F. Ghoniem, *Powder Technol.*, **316**, 500 (2017).
27. K. M. Wgialla, A. M. Helal and S. S. E. H. Elnashaie, *Math. Comput. Model.*, **15**, 17 (1991).
28. Z. Zhai, X. Wang, R. Licht and A. T. Bell, *J. Catal.*, **325**, 87 (2015).
29. R. I. Rothenberg and J. M. Smith, *AIChE J.*, **12**, 213 (1966).
30. R. Serrano-López, J. Fradera and S. Cuesta-López, *Chem. Eng. Process.*, **73**, 87 (2013).